

Optical Engineering

OpticalEngineering.SPIEDigitalLibrary.org

InAs/GaAs quantum-dot intermixing: comparison of various dielectric encapsulants

Hala H. Alhashim
Mohammed Zahed Mustafa Khan
Mohammed A. Majid
Tien K. Ng
Boon S. Ooi

SPIE.

InAs/GaAs quantum-dot intermixing: comparison of various dielectric encapsulants

Hala H. Alhashim, Mohammed Zahed Mustafa Khan,[†] Mohammed A. Majid,[‡] Tien K. Ng, and Boon S. Ooi*

King Abdullah University of Science and Technology (KAUST), Computer, Electrical and Mathematical Sciences and Engineering Division, Photonics Laboratory, Thuwal 239556900, Saudi Arabia

Abstract. We report on the impurity-free vacancy-disordering effect in InAs/GaAs quantum-dot (QD) laser structure based on seven dielectric capping layers. Compared to the typical SiO₂ and Si₃N₄ films, HfO₂ and SrTiO₃ dielectric layers showed superior enhancement and suppression of intermixing up to 725°C, respectively. A QD peak ground-state differential blue shift of >175 nm (>148 meV) is obtained for HfO₂ capped sample. Likewise, investigation of TiO₂, Al₂O₃, and ZnO capping films showed unusual characteristics, such as intermixing-control caps at low annealing temperature (650°C) and interdiffusion-promoting caps at high temperatures (≥675°C). We qualitatively compared the degree of intermixing induced by these films by extracting the rate of intermixing and the temperature for ground-state and excited-state convergences. Based on our systematic characterization, we established reference intermixing processes based on seven different dielectric encapsulation materials. The tailored wavelength emission of ~1060–1200 nm at room temperature and improved optical quality exhibited from intermixed QDs would serve as key materials for eventual realization of low-cost, compact, and agile lasers. Applications include solid-state laser pumping, optical communications, gas sensing, biomedical imaging, green–yellow–orange coherent light generation, as well as addressing photonic integration via area-selective, and postgrowth bandgap engineering. © The Authors. Published by SPIE under a Creative Commons Attribution 3.0 Unported License. Distribution or reproduction of this work in whole or in part requires full attribution of the original publication, including its DOI. [DOI: 10.1117/1.OE.54.10.107107]

Keywords: InAs/GaAs quantum dots; intermixing; annealing; impurity-free vacancy disordering; photoluminescence.

Paper 150903 received Jul. 3, 2015; accepted for publication Sep. 22, 2015; published online Oct. 16, 2015.

1 Introduction

Self-assembled InAs/GaAs quantum dots (SAQDs) grown using the Stranski–Krastanov growth mode have unleashed its practical device potential and applications. This is due to the extensive studies on its fundamental physics bearing three-dimensional (3-D) confinement over the past 30 years.^{1,2} High-performance lasers utilizing SAQDs have been realized exhibiting low-threshold current densities, higher gain, temperature insensitivity, and small chirp under direct modulation.^{3,4} Integrating SAQD laser diodes with other functional devices on the same chip to achieve a high density photonic integrated circuit (PIC) is highly desirable for broadband and telecom systems. Instead of hybrid integration based on discrete components, seamless integration of active and passive components based on monolithic integration is crucial to the success of PIC. Notably, the use of selective area postgrowth intermixing technique,^{5–8} to achieve two or more optical elements with varying transition energy, on the same quantum dot (QD) wafer,^{9,10} is attractive. Thus, capping materials for selective area intermixing need to be carefully selected for proper bandgap engineering of different regions to avoid absorption.¹¹ Also, the overlapping transition energies of the intermixed region broadens the emission bandwidth for various broadband applications such as biomedical

imaging,¹² optical communications, and so on.¹³ Furthermore, the wavelength window of ~1060–1200 nm is garnering attention because of its multitude of applications, e.g., as a source for pumping solid-state lasers,¹⁴ visible light generation,^{15,16} laser-based gas sensing,¹⁷ metrology, and so on. Hence, an intermixed InAs/GaAs QD laser in this wavelength range would be a promising candidate to challenge the currently dominant InGaAs(N)/GaAs multiple quantum well (QW) lasers and Nd-YAG-based solid-state lasers.¹⁸

Quantum-dot intermixing (QDI) is found to be more complicated than QW intermixing due to the strong influence of the shape, size, composition, and strain distribution in and around the SAQDs.^{10,19,20} Furthermore, the high sensitivity of the SAQDs to annealing parameters (temperature and duration) is very difficult to trace. So far, several SAQD intermixing techniques, such as laser radiation-induced intermixing,^{21,22} neutral ion implantation-induced intermixing,² and impurity-free vacancy disordering (IFVD),^{23,24} have been developed and studied. Among these techniques, the IFVD process has been widely used to selectively enhance the amount of intermixing for optoelectronic devices. This simple and efficient method involves depositing a dielectric cap, usually silicon dioxide (SiO₂) on the p-GaAs cladding of the laser sample. During annealing, Ga atoms out-diffuse into the SiO₂ cap thereby generating group-III vacancies (V_{III}) in the underlying semiconductor. Diffusion of V_{III} toward the active region at elevated temperature promotes atomic interdiffusion of group-III elements between the barrier and QD, and hence shifts the QD transition energy to a higher level. In addition, the different thermal expansion coefficient between the dielectric and the QD sample results

*Address all correspondence to: Boon S. Ooi, E-mail: boon.ooi@kaust.edu.sa

[†]Currently with the King Fahd University of Petroleum and Minerals (KFUPM), Electrical Engineering Department, Dhahran 31261, Saudi Arabia.

[‡]Currently with the Effat University, Electrical and Computer Engineering Department, Jeddah 21478, Saudi Arabia.

in stress accumulation at the interface during annealing. This is found to promote (when GaAs surface is compressively strained) or trap (when GaAs surface is tensile strained) the V_{III} at the interface, thus significantly affecting the intermixing process.^{9,19,25,26} As the IFVD process is essentially impurity-free, the optical loss and degradation of electrical properties resulted from extended defect and free-carrier absorptions from impurity ions can be minimized to a great extent.

In the literature, several capping materials have been reported with IFVD annealing process. For inhibiting interdiffusion, titanium oxide (TiO_2),^{27,28} aluminum (Al),²⁸ and silicon nitride (Si_3N_4) materials²⁵ were utilized. For enhancing interdiffusion, SiO_2 capping^{9,24} was used. TiO_2 film has been demonstrated to reduce intermixing due to the larger thermal expansion coefficient compared to the GaAs substrate.²⁷ Following the same argument, smaller thermal expansion coefficient of the SiO_2 film showed a larger degree of intermixing. Furthermore, the degree of intermixing was found to enhance with increasing thickness of SiO_2 film.²⁵ Since there is always a limit to the solubility of Ga in the SiO_2 film, once saturation is reached, no more Ga vacancies can be generated. Therefore, higher solubility in thicker film enhanced intermixing compared to thin film. Besides, higher stress at the capping layer/GaAs interface due to its increased thickness also favors Ga atoms out-diffusion into the SiO_2 capping. In general, these capping materials (SiO_2 , TiO_2 , Al, and Si_3N_4) are deposited by plasma-enhanced chemical vapor deposition (PECVD) or electron-beam evaporation or sputtering methods.

In this paper, a comparative study of IFVD InAs/GaAs SAQDs with PECVD grown SiO_2 and Si_3N_4 dielectric films is demonstrated in conjunction with other novel capping materials such as hafnium dioxide (HfO_2) and strontium titanate (SrTiO_3). These are grown using pulsed laser deposition (PLD), other than Al_2O_3 (aluminum oxide), TiO_2 and ZnO (Zinc oxide), which are deposited using atomic layer deposition (ALD). Low temperature photoluminescence (PL) spectroscopy on these samples revealed that HfO_2 cap induced significant blue shift in the SAQD's ground-state (GS) emission. This indicated a comparatively higher degree of intermixing compared to the SiO_2 cap. Whereas SrTiO_3 and ZnO caps behaved as control caps with reduced rate of intermixing. Furthermore, merging of GS and ES transitions was observed at high annealing temperatures from the SiO_2 , TiO_2 , and HfO_2 samples. Also, we discuss the PL observations of different capping materials versus annealing temperature, and qualitatively characterize them by extracting two degrees of intermixing parameters: (1) critical temperature (T_C), at which SAQDs GS and ES merged and (2) rate of GS peak energy shift with annealing temperature (δE). These parameters are rules for assessing the amount of interdiffusion. Generally, our systematic IFVD study provides choices from seven different dielectric caps. These choices are promising toward postgrowth bandgap engineering for fabricating selective-area bandgap tuned PICs based on SAQDs. This, likewise, provides an excellent control over the required design parameters. Moreover, realization of single state lasing (with large and differential gain) in SAQD lasers by a simple postgrowth bandgap engineering method (i.e., annealing using selected capping material at corresponding T_C might be addressed

which otherwise employ complicated gratings²⁹ or dichroic mirror³⁰ assisting techniques.

2 Experimental Method

The laser structure, shown in Fig. 1(a), is grown on Si-doped GaAs substrate in molecular beam epitaxy equipment. Figure 1(b) corresponds to the (004) bright field cross-sectional transmission electron microscopy image of our SAQD samples, where the active region consists of eight-stack QD layers. Each QD layer is covered with a thin InGaAs strain reducing layer (SRL) followed by a partially p-doped GaAs barrier. The thickness of each QD stack (QD layer, SRL, and barrier) is 40 nm. The growth temperatures of the SAQDs

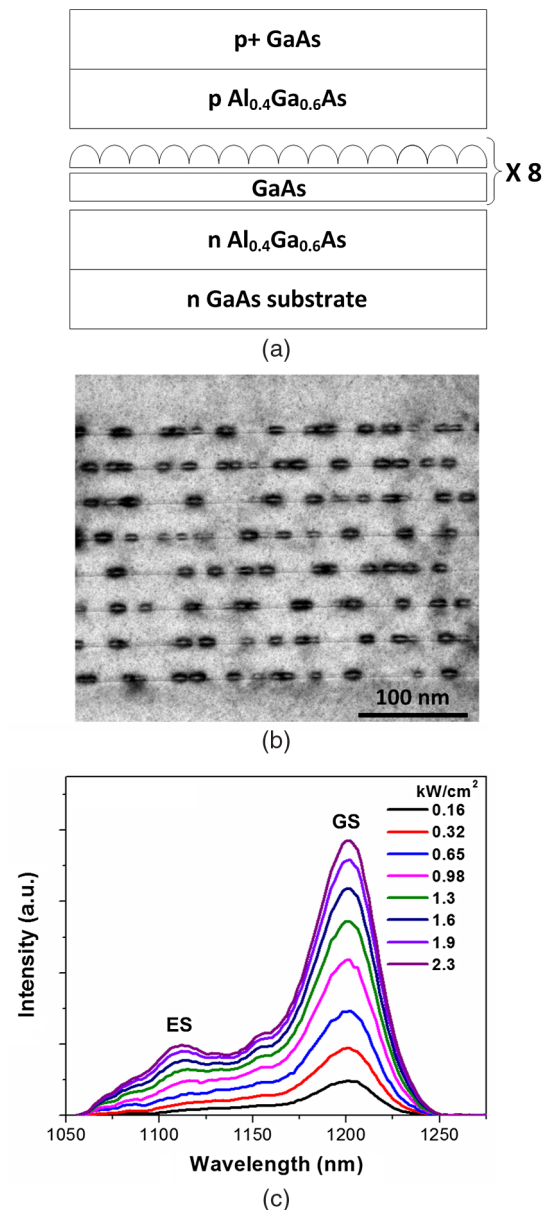


Fig. 1 Laser structures: (a) Schematic diagram of the as-grown (AG) InAs/GaAs SAQD laser structure, and the corresponding (b) cross-sectional (004) bright field transmission electron microscopy (TEM) micrograph showing the active region which comprised eight-stack quantum dot (QD) layers, and (c) the excitation power-dependent 77 K PL showing the as-grown ground-state (GS) and excited-state (ES) peaks.

and barrier layers are $\sim 500^{\circ}\text{C}$ – 525°C and $\sim 560^{\circ}\text{C}$ – 590°C , respectively. The active region is sandwiched between the n-type $\text{Al}_{0.4}\text{Ga}_{0.6}\text{As}$ lower-cladding layer and the p-type $\text{Al}_{0.4}\text{Ga}_{0.6}\text{As}$ upper-cladding layer, with a 400-nm p-type GaAs: Be contact layer. Figure 1(c) shows the excitation power-dependent low temperature (77 K) PL from the as-grown (AG) laser structure sample using 980-nm diode laser as the excitation source. At low excitation power, a single PL peak emission at 1200 nm is visible, attributed to the QD GS emission. A progressive increase in the PL emission from a high energy shoulder at 1110 nm is seen at high excitation power, which is related to the emission from the QD excited state (ES) emission besides the GS emission. An energy separation of ~ 84 meV at 77 K is observed between the two peaks, consistent with the value reported in the literature on InAs/GaAs QD material system.⁴ Henceforth, we refer the main peak intensity of any annealed sample 77 K PL spectrum as emission from GS, and the higher energy shoulder or peak as the emission from QD ES transition, for ease in discussion and calculations. We also noted another hump around ~ 1150 nm which is found to be independent of the excitation power density value, and hence we believe that this is from the fiber-based PL measurement system.

In our QDI study, seven SAQD samples are prepared using different capping materials and with various deposition techniques. They are summarized as follows: (1) 300°C PECVD of 200-nm thick SiO_2 and 100-nm thick Si_3N_4 caps; (2) 160°C ALD of 100 nm ZnO, TiO_2 , and Al_2O_3 caps; and (3) 300°C PLD of 100 nm SrTiO_3 and HfO_2 caps. Since the effect of SiO_2 capping layer thickness beyond 100 nm does not appreciably change the In–Ga intermixing process in InGaAs/GaAs SAQDs and multiple QW systems (with GS PL emission shift within an error margin of ± 15 meV). Our comparison of SiO_2 with other 100-nm thick capping layers is reasonable.^{27,31} These samples are then subjected to rapid thermal processing in nitrogen ambient at temperature values of 650°C to 725°C in steps of 25°C for 120 s, and under. As overpressure, provided by GaAs proximity cap, to minimize arsenic desorption during annealing, a fixed excitation power density of 2.3 kW/cm² is used for the rest of PL measurements to evaluate the degree of bandgap shift, and with a short wavelength detection limit of 1000 nm.

3 Results and Discussion

3.1 Plasma-Enhanced Chemical Vapor Deposition Grown SiO_2 and Si_3N_4 Caps

Figures 2(a) and 2(b) show the normalized 77 K PL spectra obtained from the PECVD SiO_2 and Si_3N_4 capped SAQD samples at different annealing temperatures. Also, PL spectrum of the AG sample is included for reference. Notice in Fig. 2(a) that increasing the annealing temperature of SiO_2 capped samples from 650°C to 725°C caused a gradual blue shift in the QD PL as compared to the AG SAQD sample. This implies IFVD facilitated Ga vacancies started to promote intermixing right from low-annealing temperatures.⁹ In addition, the PL intensity improvement (Table 1) and decrease in the PL linewidth [Fig. 2(c)] is noted, which is ascribed to the improved dot size homogeneity and reduction in the grown-in-defects due to low-temperature growth of

QDs. From Fig. 2(c), a GS differential shift of ~ 145 nm (red arrow) was observed between the AG and 725°C annealed SiO_2 sample, with associated linewidth reduction to ~ 25 nm ($\sim 40\%$ of the AG sample, obtained via Gaussian fit). The PL peak intensity improvement was also found to improve by >2 times of the AG sample, as shown in Table 1. In general, the successive QD bandgap

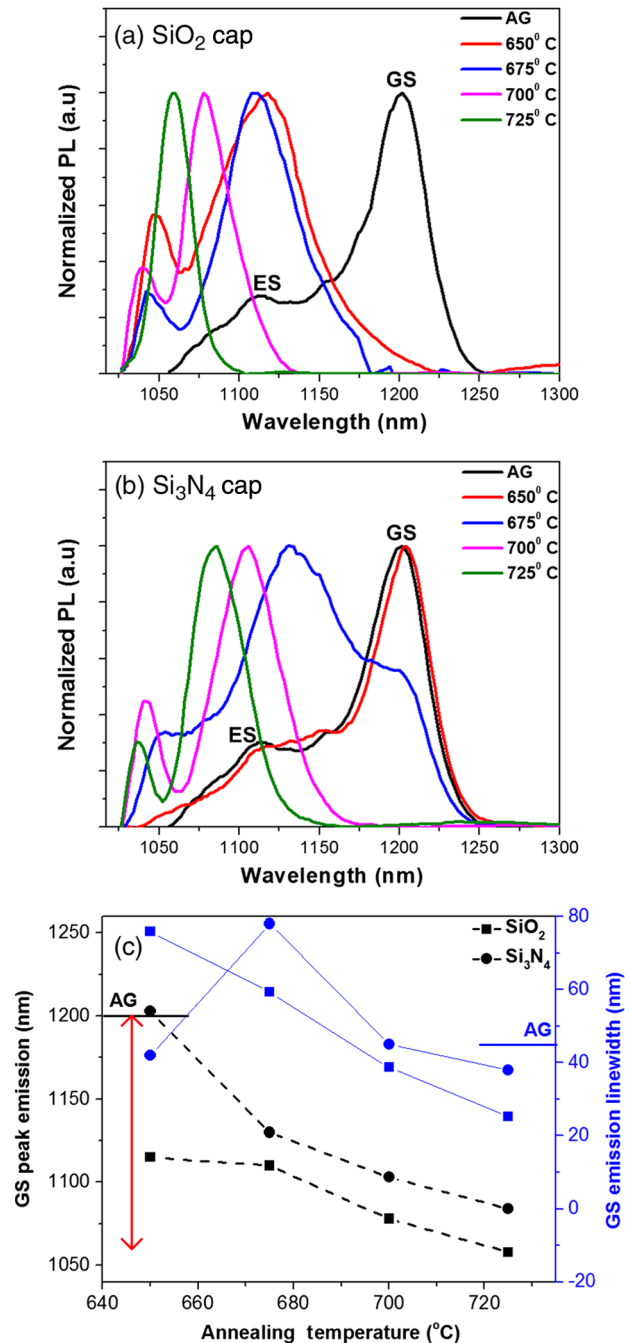


Fig. 2 Normalized 77 K photoluminescence (PL) spectra obtained from the AG and annealed samples of InAs/GaAs self-assembled InAs/GaAs quantum dots (SAQDs) at different annealing temperatures for plasma-enhanced chemical vapor deposition (PECVD) deposited: (a) SiO_2 , and (b) Si_3N_4 dielectric capping layers. Summary of the corresponding change in GS peak emission and linewidth as a function of annealing temperatures. The solid horizontal lines near both the vertical axes of (c) correspond to the as-grown values.

Table 1 Summary of the ground-state (GS) peak photoluminescence (PL) intensity and the total integrated PL intensity (shown in the parenthesis), normalized to the as-grown sample's GS peak PL intensity and the total integrated PL intensity, respectively, at different annealing temperatures and for different capping materials.

Annealing temperature (°C)	SiO ₂	Si ₃ N ₄	HfO ₂	SrTiO ₃	Al ₂ O ₃	TiO ₂	ZnO
650	0.96 (2.39)	1.11 (1.07)	1.08 (0.75)	0.81 (0.84)	0.83 (1.76)	1.17 (1.71)	0.92 (1.38)
675	1.89 (0.98)	1.15 (1.57)	2.91 (3.01)	0.97 (0.97)	— (—)	2.72 (2.36)	1.10 (1.40)
700	2.94 (2.26)	2.83 (2.33)	3.97 (1.05)	0.71 (1.02)	2.60 (2.53)	3.00 (2.13)	1.18 (1.43)
725	3.25 (1.46)	2.22 (1.55)	6.09 (1.69)	1.13 (1.57)	2.80 (2.10)	3.22 (1.83)	2.46 (1.86)

shift with increasing annealing temperature is significantly attributed to the effective sinking of Ga by SiO₂ film and enhanced vacancy diffusion deeper into the sample due to high compressive strain developed at SiO₂/GaAs interface and weakly to the thermal annealing effect. It is also worth mentioning that higher annealing temperatures reduced the intersublevel energy spacing of QD GS and ES emissions with observation of a single emission peak at 725°C, possibly due to masking of the ES emission by the dominant GS peak or by the detection limit of our PL system. However, in the case of Si₃N₄ capped sample at 725°C, as illustrated in Fig. 2(b), a clear two-peak QD PL is visible. This implies a comparatively slow interdiffusion rate offered by Si₃N₄ film and is further substantiated by an overlapping PL spectrum of 650°C annealing temperature sample with the AG sample. In other words, Si₃N₄ layer works as a control cap to partially inhibit diffusion of vacancies in the SAQD structure at this particular temperature. We postulated small group-V out-diffusion from the Si₃N₄ capped sample might be responsible for suppression of inherent thermal shift,² and negligible IFVD effect possibly due to inefficient Ga vacancies generation (insolubility of Ga or As atoms in Si₃N₄) and diffusion into the SAQD sample (smaller compressive stress at Si₃N₄/GaAs interface)²⁵ at this low temperature. Nevertheless, at 675°C and beyond, the PL spectra blue shifts in conjunction with narrow GS and ES PL linewidths, and reduction in their energy spacing, at high annealing temperatures, as depicted in Fig. 2(c). This is indicative of enhanced interdiffusion mediated through competing thermal annealing and IFVD process. Note that our observations are in agreement with most reported results^{2,27,32} on similar In(Ga)As/GaAs QD material system. These observations are in contrast to the work of Wang et al.,²³ which reported a high degree of intermixing from Si₃N₄ cap compared to SiO₂ on InAs/InGaAlAs/InP QD-in-well material system, and attributed to dominant In outdiffusion with respect to Ga. However, we believe Ga outdiffusion to be dominant in our InAs/GaAs SAQD sample. Referring to Figs. 2(a) and 2(b), it is worth mentioning that selectively intermixing SAQD sample with Si₃N₄ and SiO₂ film at 650°C may result in ultrabroad simultaneous and comparable PL emission from QD GS and ES, with -3 dB bandwidth spanning ~250 nm. Devices exhibiting such broad emissions are highly attractive for applications in optical communication, such as broadband lasers, detectors, modulators, etc.,^{22,28} discussed later in this work. In addition, a blue shifted and broad emission with peak PL intensity at ES rather than GS with linewidth of ~78 nm is observed with Si₃N₄ capped SAQD sample at

an intermediate temperature of 675°C (GS emission shoulder is still visible at ~1200 nm). In fact, analogous behavior is noticed in the PL results of other capping materials (HfO₂, Al₂O₃, ZnO, and TiO₂ caps) at low and intermediate annealing temperatures. We attribute this observation to an increased interface fluctuation between SAQDs and the surrounding matrix at low and intermediate temperatures, and possible defect annealing near the interface.^{2,33} This improved with increasing temperature as a result of higher In-Ga intermixing. The normalized integrated PL intensity and the GS peak PL intensity of Si₃N₄ and SiO₂ capping layers at different annealing temperatures are summarized in Table 1. The results suggest that the optical quality of the SAQDs is maintained at low and intermediate temperatures via possible reduction of the defect density and the non-radiative recombination centers. At relatively high annealing temperature, enhanced In-Ga intermixing resulted in improvement of the QD size distribution and the structural quality.^{20,23}

3.2 Pulsed Laser Deposition Grown HfO₂ and SrTiO₃ Caps

Figures 3(a) and 3(b) show the PL spectra of the samples capped with 100 nm PLD HfO₂ and SrTiO₃ caps at different annealing temperatures. The corresponding changes in the peak GS emission wavelength and PL linewidth are summarized in Fig. 3(c). The HfO₂ capped sample shows inhibition to intermixing at 650°C with no differential shift in the GS peak emission. The ES PL intensity is found to increase in this case, similar to the Si₃N₄ capped samples at intermediate temperature. Apart from possible defect annealing near the QD/barrier interface,² we attribute this observation to the minor outdiffusion of Ga from smaller size QDs in particular due to comparatively larger surface to volume ratio, than larger size QDs at low annealing temperatures.²³ As the temperature is increased to 675°C and to 700°C, a high degree of intermixing with a differential GS PL peak shift (compared to AG sample) of ~175 nm was noted. Moreover, observation of ~4.0 (2.5) times increase (decrease) in the GS peak PL intensity (linewidth) compared to the AG sample further substantiate this material being a highly efficient intermixing cap, as summarized in Table 1. Note that IFVD effect saturated at 700°C with no further blue shifting of the GS photoluminescence peak beyond this annealing temperature. Moreover, a single peak emission at 725°C possibly indicates merging of GS and ES emissions. The PL linewidth at this annealing temperature was found to be similar in value (~18 nm) compared to the 700°C annealed sample except

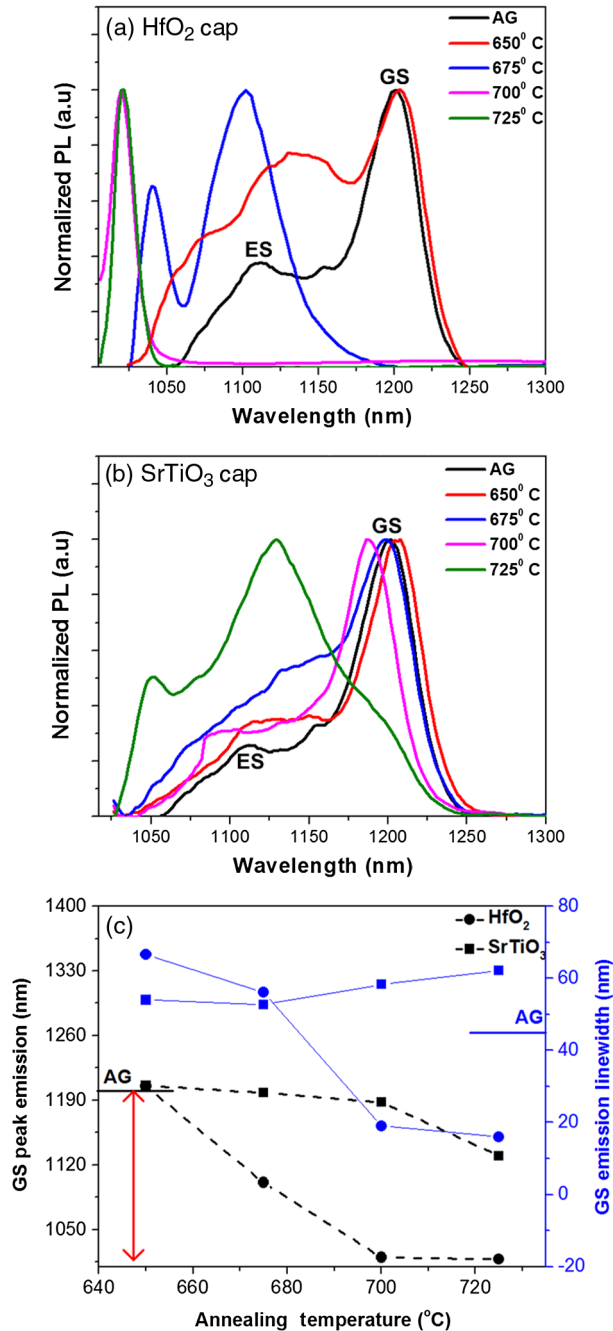


Fig. 3 Normalized 77 K PL spectra obtained from the as-grown and annealed samples of InAs/GaAs SAQDs at different annealing temperatures for pulsed laser deposition (PLD) deposited: (a) HfO₂, and (b) SrTiO₃ dielectric capping layers. Summary of the corresponding change in GS peak emission and linewidth as a function of annealing temperatures. The solid horizontal lines near both the vertical axes of (c) correspond to the as-grown values.

with an increase in the peak PL intensity ($\sim 50\%$) and comparable integrated PL intensity. This might be due to complete inhabitation of intrinsic defects, possible oxygen vacancies, in the 100-nm thick HfO₂ film by Ga outdiffusion.³⁴ In addition, the alteration of strain at the HfO₂/GaAs interface (possibly from thermal matching to tensile strained GaAs surface region) at elevated annealing temperatures could also play a role in suppressing the interdiffusion process.^{27,32} A selection of a thick HfO₂ capping

layer would probably enable observation of intermixing effect beyond 700°C. In general, annealing SAQD samples with SiO₂ and HfO₂ caps enhanced the QD luminescence with spectral narrowing and has been attributed to the improvement in the QD inhomogeneity. On the contrary, dissolving of QDs into QD-QW metamorphic structure (two-dimensional-like system) at high temperatures is also possibly due to strong lateral In–Ga interdiffusion in the 3-D QD structures, and might lead to improved material quality, as indicated in Refs. 28 and 35. In either case, an emission window of 1030–1060 nm at 77 K translates to ~ 1100 –1160 nm at room temperature. Hence, employing high temperature ($>700^\circ\text{C}$) annealed SiO₂ or HfO₂ capped SAQD lasers with superior characteristics would enable realization of frequency-doubled green–orange–yellow band lasers.¹⁵ Alternatively, SAQDs deposited with the SrTiO₃ film are found to be a highly effective cap for intermixing suppression, as depicted in Fig. 3(b). A remarkable inhibition to the thermal shift and Ga vacancy diffusion up to 700°C is demonstrated with a mere ~ 16 nm GS differential shift compared to the AG sample. Moreover, the PL intensity and the PL linewidth are found to be analogous to the AG sample, thus representative of preserving the optical quality of the annealed samples, as depicted in Table 1. We postulate that a high degree of tensile stress created at the SrTiO₃/GaAs interface impede the down diffusion of Ga vacancies and thus inhibit group-III intermixing between QDs and surrounding barrier layers. A large thermal expansion coefficient of the SrTiO₃ cap, which is $\sim 22\%$ larger than the typical TiO₂ cap, further upholds our postulation.²⁷ On the other hand, SrTiO₃ may also cause reduction of Ga vacancies generation possibly due to various factors during annealing such as layer quality, diffusion of inherent defects, and the metallurgical reaction between GaAs and SrTiO₃ films.³² Note that, at 725°C, a PL blue shift accompanied by a broad emission with peak at ES rather than GS (shoulder at longer wavelength region) is observed, indicating that the limit for intermixing inhibition is up to 700°C. We postulate that the emission peaks observed at 1125 and 1050 nm is from the GS and ES of highly interdiffused QDs with small sizes, and the long wavelength shoulder to the GS emission of least interdiffused QDs with larger size where the interdiffusion is minimal. We also believe that the shift in the GS peak emission wavelength at 725°C is also controlled by the intrinsic thermal annealing induced disordering effect.²

3.3 Atomic Layer Deposition Grown Al₂O₃, ZnO, and TiO₂ Caps

Low temperature PL spectra of ALD deposited Al₂O₃, ZnO, and TiO₂ capped SAQD samples at annealing temperatures from 650°C to 725°C are plotted in Figs. 4(a)–4(c), respectively. For all capping materials, we observed inhibition of intermixing at a low-annealing temperature of 650°C, similar to the Si₃N₄, HfO₂, and SrTiO₃ caps, and the same reason holds for these ALD grown dielectric films. As the annealing temperature is increased beyond 650°C, a progressive blue shift in the GS peak PL emission is observed in all three (Al₂O₃, ZnO, and TiO₂) samples, as shown in Fig. 4(d). In all the cases, an improvement in the material quality is noted and summarized in Table 1. However, GS and ES peaks did not merge in all the three capped samples even

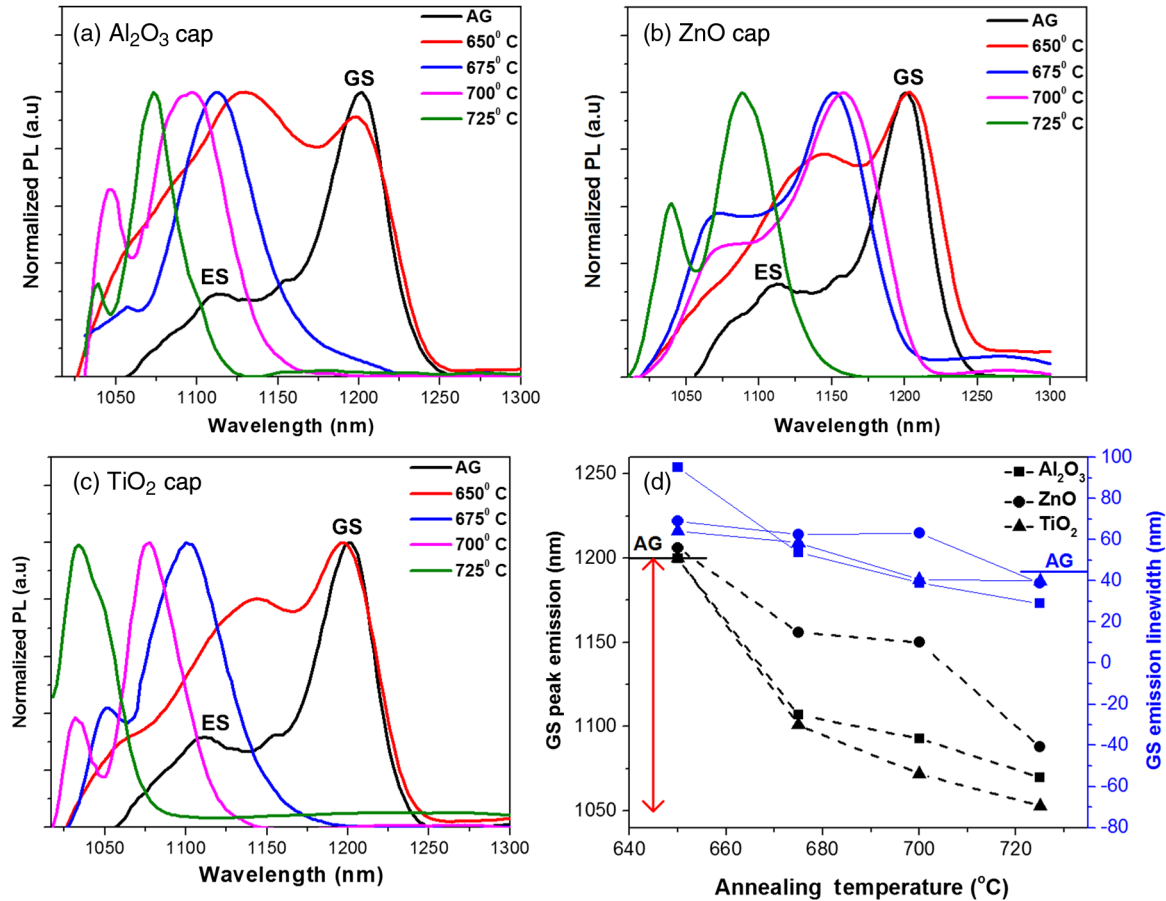


Fig. 4 Normalized 77 K PL spectra obtained from the as-grown and annealed samples of the InAs/GaAs QDs at different annealing temperatures for atomic layer deposition (ALD) deposited: (a) Al₂O₃, (b) ZnO, and (c) TiO₂. Summary of the corresponding change in GS peak emission and linewidth as a function of annealing temperatures. The solid horizontal lines near both the vertical axes of (d) correspond to the as-grown values.

at the highest annealing temperature of 725°C. Distinct peak emissions from both the transition states are clearly observed in Al₂O₃ and ZnO capped samples, whereas the TiO₂ capped sample showed bimodal peak behavior, a result of reduction in the intersublevel energy spacing of QD GS and ES emissions. Nonetheless, the TiO₂ film showed the highest degree of intermixing when compared to the other two ALD films with a GS peak blue shift of ~165 nm and similar PL linewidth value compared to the AG data, as elaborated in Fig. 4(d). This observation is most likely due to our ALD technique that might alter the film porosity and thus promote intermixing,²⁵ as compared to the literature^{27,28} where e-beam evaporated TiO₂ film was shown to inhibit intermixing. On the other hand, 675°C and 700°C annealed ZnO capped samples showed a small GS wavelength blue shift of ~32 nm compared to the AG sample indicative of partial inhibition of the IFVD process. However, the GS PL linewidth broaden at this temperature by ~40% (compared to the AG sample) and is accompanied by increased luminescence from the ES of QDs. This suggests increased QD size and composition dispersion as observed in other PECVD and ALD samples. In general, at low-annealing temperatures (650°C and 675°C) most of the capping layers showed increased GS PL linewidth, which has been

attributed to the interface fluctuation between SAQDs and the surrounding matrix, thus affecting the QD transition states. In addition, an inhomogeneous rate of In–Ga diffusion in different QD sizes given 3-D and complex intermixing process could also be ascribed for this observation.² In the case of the Al₂O₃ capped sample, typical blue shifting of the GS peak wavelength is observed with progressive narrowing and enhancement of the PL linewidth and intensity, respectively, with a maximum peak shift of ~125 nm at 725°C compared to the reference AG data. In general, this layer behaves similar to the other IFVD promoting caps (SiO₂, HfO₂, and Al₂O₃) and retains (improves) the optical quality of the material after low (high) temperature annealing, as illustrated in Table 1. A remarkable observation that is worth mentioning about this film is the broadened emission with equal intensities from both GS and ES transitions of QDs annealed at low temperature (650°C), indicating increased compositional fluctuation at the interface between the QD and the surrounding matrix as compared to TiO₂ and ZnO capping, leading to a dispersive QD potential profiles, in particular, affecting the smaller dots with higher intermixing rate as discussed earlier.³⁶ An ultrabroad PL linewidth of ~165 nm from this single capped low-temperature intermixed SAQD structure, centered at ~1140 nm

is again highly attractive for biomedical imaging, in the low-coherence interferometry system such as optical coherence tomography.^{13,22}

3.4 Comparative Analysis

To compare the performance of different capping layers, we extracted two parameters that characterize their degree of intermixing, namely the intermixing rate (δE) and the critical temperature (T_C). Figures 5(a)–5(c) and 6(a)–6(c) show the GS peak energy shift, and the energy separation between GS and ES (ΔE), extracted from the 77 K PL spectra, as a

function of annealing temperature, and corresponding to PECVD, PLD, and ALD deposited capping materials, respectively. The results are summarized in Table 2. For simplicity in analysis, we selected the region that showed linear interdiffusion (promotion by all the samples except SrTiO₃ and ZnO which showed inhibition of interdiffusion) and ΔE behavior, for estimating δE and T_C ,^{9,24} respectively, with $\pm 20^\circ\text{C}$ margin of error in the latter case (ΔE values are extracted from GS and ES Gaussian fittings). A reasonably good linear fitting is obtained in both the parameter extraction cases, as depicted in Figs. 5 and 6, with close agreement

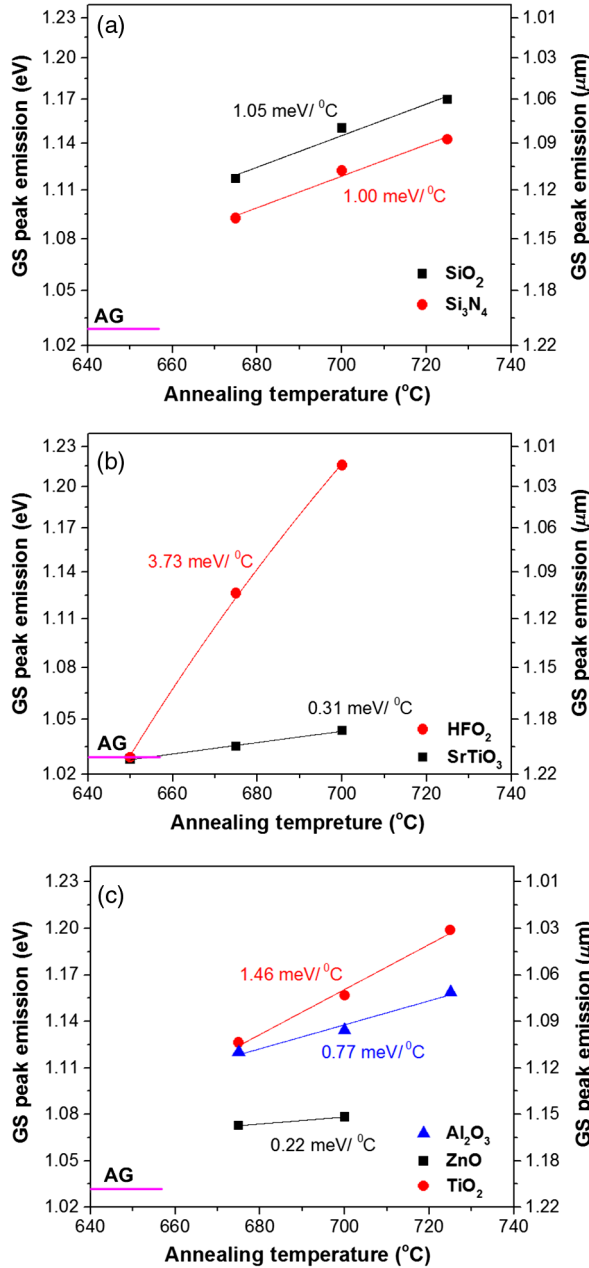


Fig. 5 Linear fitting of the GS peak energy shift as a function of annealing temperatures: (a) PECVD grown SiO₂ and Si₃N₄, (b) PLD grown HfO₂ and SrTiO₃, and (c) ALD grown Al₂O₃, TiO₂, and ZnO capped InAs/GaAs SAQD structure, respectively. The slope of the linear fit provides the rate of interdiffusion δE . The solid horizontal line near the vertical axis corresponds to the as-grown GS peak energy.

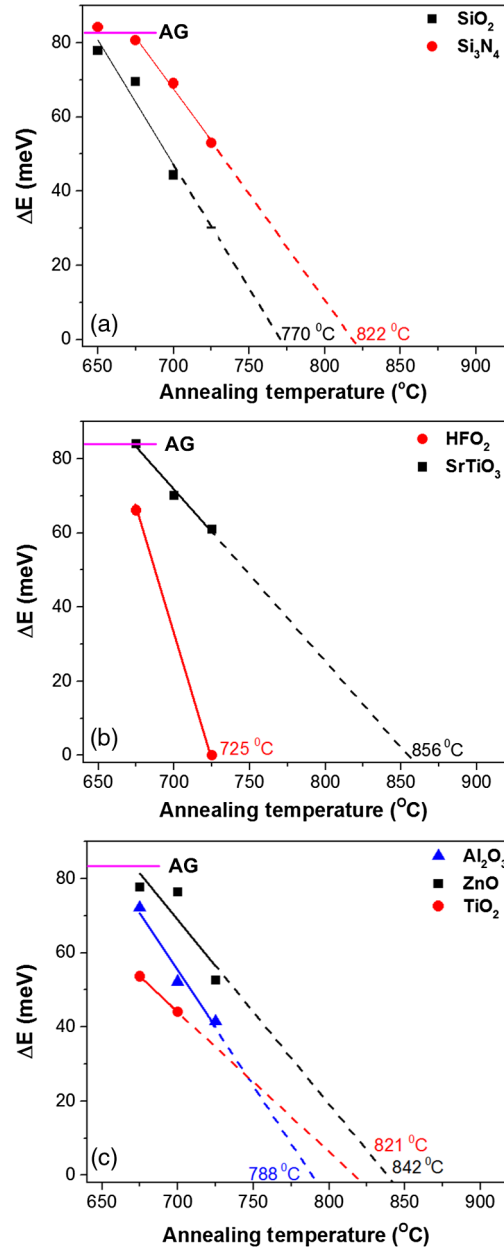


Fig. 6 Linear fitting of the GS and ES peak energy separation as a function of annealing temperatures: (a) PECVD grown SiO₂ and Si₃N₄, (b) PLD grown HfO₂ and SrTiO₃, and (c) ALD grown Al₂O₃, TiO₂, and ZnO capped InAs/GaAs SAQD structure, respectively. The critical temperature T_C is calculated by subsequent linear extrapolation. The solid horizontal line near the vertical axis corresponds to the AG ΔE value.

Table 2 Summary of the extracted δE and T_C values of different IFVD processed InAs/GaAs SAQD capping materials.

Capping material	Growth technique	DOI parameters	
		δE (meV/°C)	T_C (°C)
SiO ₂	PECVD	1.05	770
Si ₃ N ₄	PECVD	1.00	822
HfO ₂	PECVD	3.73	725
SrTiO ₃	PLD	0.31	856
Al ₂ O ₃	PLD	0.77	788
TiO ₂	ALD	1.46	821
ZnO	ALD	0.22	842

of T_C value obtained from linear interpolation and the experiments. For instance, possible merging of QD GS and ES emissions is observed in HfO₂ and with some uncertainty in SiO₂ and Al₂O₃ capped samples, at 725°C; meanwhile, the corresponding extracted T_C values are 725°C, 770°C, and 788°C, respectively. The rate of intermixing is found to be highest for the HfO₂ film with $\delta E = 3.7$ meV/°C and $T_C = 725$ °C. Compared to SiO₂ film, an increase in δE by a factor of more than 3 (1.05 meV/°C for SiO₂) with similar T_C values is noted. This suggests that PLD HfO₂ cap has better capability to promote In–Ga interdiffusion between barrier layers and QDs compared to PECVD SiO₂ cap. A similar increase in δE value (by a factor of 2.5–4.5) is also observed on comparing HfO₂ capped sample with other IFVD promoting caps, i.e., ALD deposited TiO₂ (1.46 meV/°C) and Al₂O₃ (0.77 meV/°C) films; the latter also showing a relatively higher degree of intermixing with larger (smaller) δE (T_C) values. Most likely this observation might be attributed to the quality of the capping layer with possible increase in porosity for the PLD film compared to ALD caps, which changes the interdiffusion rate.²⁵ In contrast, the extracted slope of the linear fit for PLD SrTiO₃ capped sample data (within the linear region) with value $\delta E = 0.31$ meV/°C and covering higher annealing temperatures signifies strong IFVD inhibition compared to ZnO (0.22 meV/°C but obtained with smaller annealing temperature range) and Si₃N₄ (1.00 meV/°C) caps with similar predicted T_C value of 856°C (compared to 842°C and 822°C, respectively). Thus, SrTiO₃ is more attractive due to its ability to inhibit intermixing within a larger and higher range of annealing temperatures. Note that Si₃N₄ dielectric layer, in our case, behaved more as an intermixing-induced film rather than an inhibiting cap at high-annealing temperatures, and is found to be in good agreement with other reports.^{2,10,23} The possible reason for this efficient control of QD emission during IFVD process by SrTiO₃ is the large tensile stress created at the surface, more than a factor of 2, compared to the ZnO and Si₃N₄ caps. Therefore, this possibly resulted in more effective defect agglomeration and cluster formation.² The δE value of SrTiO₃ is found to be one order of magnitude smaller than HfO₂ cap, providing a differential bandgap shift of ~ 175 nm between them. We also observed that in spite of the δE value being similar for Al₂O₃, TiO₂,

Si₃N₄, and SiO₂ ($\sim 1.0 \pm 0.3$ meV/°C) capped samples, the extracted T_C values of TiO₂ and Si₃N₄ films are found to be larger than the other capping layers. We postulate that the increased outdiffusion of Ga from small dots (dominating the ES emission) as compared to the larger dots (dominating the GS emission) might be responsible for this observation.

3.5 Applications

Our analysis of characterizing the degree of intermixing via δE and T_C qualitatively provided a series of data to exploit seven different capping layers as interdiffusion suppressors or promoters for various applications. In the following, we highlight three potential applications employing either one or a combination of different caps:

- i. Bandgap engineered GS peak differential shift of ~ 35 meV between 675°C annealed HfO₂ (or SiO₂), ZnO, and SrTiO₃ capping layers could possibly be utilized in photonic integration for lasers (detectors), electro-absorption modulators, and waveguide (combiners), respectively, thus enabling various benefits such as excellent alignment, negligible reflection losses, and intrinsic mode matching.^{5,6,11} Besides, a larger GS differential bandgap shift of ~ 50 and ~ 80 meV could also be achieved using HfO₂–Al₂O₃–SrTiO₃ combination at 700°C and 725°C annealing temperatures, respectively.
- ii. Ultrabroadband devices (superluminescent diodes, laser diodes, SOA, photo detectors, modulators, etc.) might be realized employing multiple caps combination in addition to a single Al₂O₃ (650°C); for instance, a combination of SrTiO₃–ZnO–Al₂O₃–HfO₂ at 700°C would provide a possible emission bandwidth of ~ 200 nm centered at ~ 1100 nm. These ultrabroadband components are highly attractive for applications in optical communications, short pulse generation, tunable lasers, etc.,^{4,28,37} besides serving as attractive compact broadband light sources for biomedical imaging.^{13,33}
- iii. Postgrowth wavelength tuned SAQD lasers with 725°C annealed SiO₂ or HfO₂ or TiO₂ caps, with lasing wavelengths in ~ 1060 – 1200 nm range, could potentially provide high power wide green–yellow–orange band coherent light by intracavity frequency doubling^{15,16} and use in picoprojectors. Moreover, the distinct advantages of reduced threshold current density, temperature sensitivity, filamentation, and mirror degradation in QD lasers will enable realization of high-performance devices in this wavelength range compared to their InGaAs/GaAs and InGaNaNs/GaAs multiple-QW laser counterparts.¹⁸ Moreover, a bandgap tuned ~ 1064 nm QD laser could be used for injection seeding of a typical Nd-Yag 1064-nm solid-state laser¹⁴ or as a substitute because of its small footprint, high power, and comparatively superior performance. The field of metrology and gas sensing would also benefit from the bandgap tuned ~ 1060 – 1200 nm QD laser diodes in detection of water; HBr, HI, HCl molecules; ethanol and water in gasoline, etc.; for process and environmental control.^{17,38} The low atmospheric absorption window of ~ 1000 – 1100 nm will also enable deployment of postgrowth bandgap tuned QD lasers in light detection

and ranging systems where currently 1064-nm Nd-YAG lasers dominate,³⁹ along with free-space optical communications.

4 Conclusion

We have demonstrated the viability of the IFVD process on InAs/GaAs SAQDs by various dielectric capping materials with emission wavelength trimming to ~1100–1200 nm for potential realization in photonics integrated circuits and postgrowth wavelength tuned optoelectronic devices. Compared with the traditional dielectric capping layers, we presented HfO₂ and SrTiO₃ as potential candidates for tailoring the bandgap properties of QDs with superior optical properties. The corresponding extracted interdiffusion rates in these materials were found to be 3.73 and 0.31 meV/°C. This is significantly higher than common SiO₂ and Si₃N₄ dielectric films. Moreover, assessment of other uncommon dielectric capping layers such as TiO₂, Al₂O₃, and ZnO were also performed showing attractive features, and thus increasing the flexibility in capping layer selection for selective bandgap engineering for a plethora of multidisciplinary applications. In general, all the films exhibited linewidth narrowing and peak/integrated PL intensity improvement after annealing thus suggesting enhanced material quality.

Acknowledgments

This work was supported by King Abdullah University of Science and Technology's Baseline Funding and Competitive Research under Grant No. CRG-1-2012-OOI-010.

References

1. D. Bimberg, M. Grundmann, and N. N. Ledentsov, *Quantum Dot Heterostructures*, John Wiley & Sons, England (1999).
2. H. S. Djie, B. S. Ooi, and V. Aimez, "Neutral ion-implantation-induced selective quantum-dot intermixing," *Appl. Phys. Lett.* **87**, 261102 (2005).
3. M. Stubenrauch et al., "15 Gb/s index-coupled distributed-feedback lasers based on 1.3 μm InGaAs quantum dots," *Appl. Phys. Lett.* **105**, 011103 (2014).
4. A. Zhukov, M. Maksimov, and A. Kovsh, "Device characteristics of long-wavelength lasers based on self-organized quantum dots," *Semiconductors* **46**, 1225–1250 (2012).
5. J. H. Marsh, "Quantum well intermixing," *Semicond. Sci. Technol.* **8**, 1136 (1993).
6. B. S. Ooi et al., "Selective quantum-well intermixing in GaAs-AlGaAs structures using impurity-free vacancy diffusion," *IEEE J. Quantum Electron.* **33**, 1784–1793 (1997).
7. V. Aimez et al., "Low-energy ion-implantation-induced quantum-well intermixing," *IEEE J. Sel. Top. Quantum Electron.* **8**, 870–879 (2002).
8. B. S. Ooi, T. K. Ong, and O. Gunawan, "Multiple-wavelength integration in InGaAs-InGaAsP structures using pulsed laser irradiation-induced quantum-well intermixing," *IEEE J. Quantum Electron.* **40**, 481–490 (2004).
9. D. Bhattacharyya et al., "Selective control of self-organized In 0.5 Ga 0.5 As/GaAs quantum dot properties: quantum dot intermixing," *J. Appl. Phys.* **88**, 4619–4622 (2000).
10. P. Lever et al., "Impurity free vacancy disordering of InGaAs quantum dots," *Proc. SPIE* **4656**, 43–48 (2002).
11. H. Susanto Djie et al., "Quantum dash intermixing," *IEEE J. Sel. Top. Quantum Electron.* **14**, 1239–1249 (2008).
12. P. Judson et al., "Maximising performance of optical coherence tomography systems using a multi-section chirped quantum dot superluminescent diode," *Microelectron. J.* **40**, 588–591 (2009).
13. Z. Zhang et al., "Self-assembled quantum-dot superluminescent light-emitting diodes," *Adv. Opt. Photonics* **2**, 201–228 (2010).
14. W. Zeller et al., "High-power pulsed 976-nm DFB laser diodes," *Proc. SPIE* **7682**, 76820T (2010).
15. F. Heinrichsdorff et al., "High-power quantum-dot lasers at 1100 nm," *Appl. Phys. Lett.* **76**, 556–558 (2000).
16. E. Pavelescu et al., "1100 nm InGaAs/(Al) GaAs quantum dot lasers for high-power applications," *J. Phys. D: Appl. Phys.* **44**, 145104 (2011).
17. W. Zeller et al., "DFB lasers between 760 nm and 16 μm for sensing applications," *Sensors* **10**, 2492–2510 (2010).
18. L. Fan et al., "Highly strained InGaAs/GaAs multiwatt vertical-external-cavity surface-emitting laser emitting around 1170 nm," *Appl. Phys. Lett.* **91**, 1114 (2007).
19. L. Fu et al., "Study of intermixing in InGaAs/(Al)GaAs quantum well and quantum dot structures for optoelectronic/photonics integration," *IEEE Proc. Circuits Devices Syst.* **152**, 491–496 (2005).
20. Q. Cao et al., "Effects of rapid thermal annealing on optical properties of p-doped and undoped InAs/InGaAs dots-in-a-well structures," *J. Appl. Phys.* **104**, 033522 (2008).
21. V. Yakovlev et al., "Laser-induced phase transformations in semiconductor quantum dots," *Appl. Phys. Lett.* **76**, 2050–2052 (2000).
22. C. K. Chia et al., "Ultrawide band quantum dot light emitting device by postfabrication laser annealing," *Appl. Phys. Lett.* **90** (2007).
23. Y. Wang, H. Djie, and B. Ooi, "Group-III intermixing in InAs/InGaAlAs quantum dots-in-well," *Appl. Phys. Lett.* **88**, 111110 (2006).
24. C. Chia et al., "Impurity free vacancy disordering of InAs/GaAs quantum dot and InAs/InGaAs dot-in-a-well structures," *Thin Solid Films* **515**, 3927–3931 (2007).
25. P. Lever, H. H. Tan, and C. Jagadish, "Impurity free vacancy disordering of InGaAs quantum dots," *J. Appl. Phys.* **96**, 7544–7548 (2004).
26. T. Ng et al., "Thermally induced diffusion in GaInNAs/GaAs and GaInAs/GaAs quantum wells grown by solid source molecular beam epitaxy," *J. Appl. Phys.* **97**, 013506 (2005).
27. L. Fu et al., "Suppression of interdiffusion in InGaAs/GaAs quantum dots using dielectric layer of titanium dioxide," *Appl. Phys. Lett.* **82**, 2613–2615 (2003).
28. K. J. Zhou et al., "Quantum dot selective area intermixing for broadband light sources," *Opt. Express* **20**, 26950–26957 (2012).
29. C. S. Lee et al., "Characteristics of a high speed 1.22 μm tunnel injection p-doped quantum dot excited state laser," *Appl. Phys. Lett.* **98**, 011103 (2011).
30. D. Arsenijević et al., "Comparison of dynamic properties of ground- and excited-state emission in p-doped InAs/GaAs quantum-dot lasers," *Appl. Phys. Lett.* **104**, 181101 (2014).
31. J. S. Yu et al., "Effects of the thickness of dielectric capping layer and the distance of quantum wells from the sample surface on the intermixing of In_{0.2}Ga_{0.8}As/GaAs multiple quantum well structures by impurity-free vacancy disordering," *J. Korean Phys. Soc.* **42**, S458–S461 (2003).
32. L. Fu et al., "Suppression of interdiffusion in GaAs/AlGaAs quantum-well structure capped with dielectric films by deposition of gallium oxide," *J. Appl. Phys.* **92**, 3579–3583 (2002).
33. Z. Zhang et al., "Realization of extremely broadband quantum-dot superluminescent light-emitting diodes by rapid thermal-annealing process," *Opt. Lett.* **33**, 1210–1212 (2008).
34. T. Lin et al., "Impurity free vacancy diffusion induced quantum well intermixing based on hafnium dioxide films," *Mater. Sci. Semicond. Process.* **29**, 150–154 (2014).
35. A. Babiński et al., "Rapid thermal annealing of InAs/GaAs quantum dots under a GaAs proximity cap," *Appl. Phys. Lett.* **79**, 2576–2578 (2001).
36. Z. Y. Zhang et al., "Effects of intermixing on modulation p-doped quantum dot superluminescent light emitting diodes," *Opt. Express* **18**, 7055–7063 (2010).
37. H. Djie et al., "Room-temperature broadband emission of an InGaAs/GaAs quantum dots laser," *Opt. Lett.* **32**, 44–46 (2007).
38. S. H. Hwang et al., "Detection wavelength tuning of InGaAs/GaAs quantum dot infrared photodetector with thermal treatment," *Microelectron. J.* **36**, 203–206 (2005).
39. Y. Hu et al., "Sea surface wind speed estimation from space-based lidar measurements," *Atmos. Chem. Phys.* **8**, 3593–3601 (2008).

Hala H. Alhashim is a PhD candidate in the material science and engineering program since September 2011 at King Abdullah University of Science and Technology (KAUST). In 2007, she received her master's degree in physics from the King Faisal University and later worked as an instructor in the Physics Department, Dammam University for 9 years. Her research interests include superconductor materials, solid-state physics, and photonics, particularly in bandgap engineering of quantum well/quantum-dot (QD) semiconductor materials.

Mohammed Zahed Mustafa Khan received his PhD in electrical engineering from King Abdullah University of Science and Technology (KAUST), Saudi Arabia, in 2013. Currently, he is an assistant professor at King Fahd University of Petroleum and Minerals (KFUPM), Saudi Arabia. Prior to earning his PhD, he worked as a lecturer at KFUPM from 2004 to 2009. His primary research involves the

theoretical and experimental work on quantum confined nanostructure lasers, particularly on broadband quantum-dash lasers.

Mohammed A. Majid received his PhD in electronic and electrical engineering from University of Sheffield, UK, in 2011, before working as an EPSRC postdoctoral fellow for a year in the field of photonics. From 2012 to 2015, he continued as a postdoctoral fellow in the electrical engineering program at King Abdullah University of Science and Technology (KAUST), Saudi Arabia. Currently, he is an assistant professor in the Electrical and Computer Engineering Department, Effat University, Saudi Arabia.

Tien K. Ng received his PhD in electrical and electronics engineering from Nanyang Technological University (NTU), Singapore, in 2005. He was a member of the technical staff with Tinggi Technologies,

Singapore, from 2004 to 2006, and later a research fellow at NTU until 2009. Currently, he is a research scientist at King Abdullah University of Science and Technology (KAUST), Saudi Arabia, and the co-principal investigator for the technology innovation center for solid-state lighting at KAUST.

Boon S. Ooi received his PhD in electronics and electrical engineering from the University of Glasgow, UK. He served as a faculty member at Nanyang Technological University (Singapore) and Lehigh University (USA) before he joined the King Abdullah University of Science and Technology as a professor of electrical engineering in 2009. His research interests include semiconductor lasers and photonics integrated circuits. He is a fellow of SPIE and the Institute of Physics, UK.